8-2008

A Validation Study for the Hydrodynamics of Biomass in a Fluidized Bed

Mirka Deza
Virginia Polytechnic Institute and State University, mdeza@iastate.edu

Francine Battaglia
Virginia Polytechnic Institute and State University

Theodore J. Heindel
Iowa State University, theindel@iastate.edu

A Validation Study for the Hydrodynamics of Biomass in a Fluidized Bed

Abstract

Computational modeling of fluidized beds can be used to predict operation of biomass gasifiers after extensive validation with experimental data. The present work focused on computational simulations of a fluidized bed using a multifluid Eulerian-Eulerian model to represent the gas and solid phases as interpenetrating continua. Hydrodynamic results from the simulations were quantitatively compared with X-ray flow visualization studies of a similar bed. It was found that the Gidaspow model can accurately predict the hydrodynamics of the biomass in a fluidized bed. The coefficient of restitution of biomass was fairly high and did not affect the hydrodynamics of the bed; however, the model was more sensitive to particle sphericity variation.

Keywords

hydrodynamics, biomass, fluidized bed

Disciplines

Acoustics, Dynamics, and Controls | Biochemical and Biomolecular Engineering | Computer-Aided Engineering and Design | Fluid Dynamics

FEDSM2008-55158

A VALIDATION STUDY FOR THE HYDRODYNAMICS OF BIOMASS IN A FLUIDIZED BED

Mirka Deza, Francine Battaglia*
Mechanical Engineering Department
Virginia Polytechnic Institute and State University
Blacksburg, Virginia 24061

Theodore J. Heindel
Mechanical Engineering Department
Iowa State University
Ames, Iowa 50011

ABSTRACT

Computational modeling of fluidized beds can be used to predict operation of biomass gasifiers after extensive validation with experimental data. The present work focused on computational simulations of a fluidized bed using a multifluid Eulerian-Eulerian model to represent the gas and solid phases as interpenetrating continua. Hydrodynamic results from the simulations were quantitatively compared with X-ray flow visualization studies of a similar bed. It was found that the Gidaspow model can accurately predict the hydrodynamics of the biomass in a fluidized bed. The coefficient of restitution of biomass was fairly high and did not affect the hydrodynamics of the bed; however, the model was more sensitive to particle sphericity variation.

NOMENCLATURE

d Particle diameter
e Coefficient of restitution
g Gravitational acceleration
q Diffusive flux of granular energy
$\mathbf{u}$ Velocity vector
t time
C Fluctuation in the particle velocity
C_D drag coefficient
F Force
I Interphase momentum transfer
N Particle number
P Pressure
R Interphase mass transfer due to chemical reaction or physical processes
Re Reynolds number
S Stress tensor of gas or solid
U Fluidization velocity
V Velocity of gas or solid

Greek Letters

ε Void fraction
φ Blend function
γ Rate of granular energy dissipation due to inelastic collisions
μ Dynamic viscosity
ρ Density of gas or solid
σ Stress tensors
ψ Particle sphericity
Φ Granular energy transfer between gas and solid phases
θ Granular temperature

Superscripts/Subscripts

b   Bulk
g   Gas phase
i   Index of particles
l l^{th} solid phase
m m^{th} solid phase
mf   Minimum fluidization
p   Particle
s   Solid phase

---

*Corresponding author: fbattaglia@vt.edu

INTRODUCTION

Fluidized bed gasifiers are used to convert feedstock with low-carbon content into valuable products such as fuels, basic chemicals, and hydrogen. One example is the use of biomass as the feedstock in gasifiers. A current challenge is designing and constructing biomass gasifiers to supply energy for the renewable fuels industry, e.g., grain ethanol plants. There is usually a notable difference in the fluidization behavior between the solid fuel particle and the fluidized bed media (typically refractory sand) due to contrasting size, shape, and particle density. The differences can lead to poor solid fuel distribution and diminished gasifier performance. As fluidized bed reactors are scaled-up to industrial sizes, the solid fuel distribution becomes even more critical. Therefore, it is important to gain a fundamental understanding of particle mixing in fluidized beds to improve gasifier performance and optimize product output. Computational modeling of fluidized beds can be used to predict operation of biomass gasifiers after extensive validation with experimental data.

Given the nature of biomass particles (shape, moisture content, pliability), their fluidization characteristics are of critical importance because of known problems such as particle agglomeration, defluidization, elutriation, and segregation. Ideally, experiments can provide information on the fluidization characteristics of biomass but the opacity of the bed material impedes visualization techniques. Since fluidization is a dynamic process, invasive monitoring methods can influence the internal flow, thereby reducing the reliability of the measurements [1]. Currently, there are only a few instances of noninvasing monitoring techniques used for monitoring fluidized beds [2–4]. Franka et al. [4] used X-ray computed tomography and radiography to analyze differences in materials for fluidized beds operating under three gas flow rates. The CT images showed that glass beads fluidize much more uniformly compared to melamine, walnut and corncob beds and that walnut shell fluidize more uniformly as gas flow rate was increased.

Several drag models have been reported in the literature to account for the gas-solid hydrodynamics of fluidized beds. Taghipour et al. [5] compared the Syamlal-O'Brien, Gidaspow, and Wen-Yu models with experimental data and found that for relatively large Geldart B particles, the models predicted the hydrodynamics of the bed reasonably well. Du et al. [6] studied five drag models in a spouted fluidized bed and found that for dense phase simulations the models produced noticeable differences. Among the five drag models Du et al. tested, the Arastoopour and Syamlal-O'Brien models gave good predictions of the flow, but the Gidaspow drag model gave the best agreement with the experimental data. Another extensive model comparison in fluidized beds was made by Mahinpey et al. [7], for bed expansion and pressure drop with different superficial velocities in a fluidized bed. Results for the adjusted models of Syamlal–O'Brien and Di Felice showed an improvement in quantitative predictions of the bed hydrodynamics.

Using an appropriate drag model is of particular interest to the research herein. The underlying issue is that many of the drag models cited previously require information about the particle hydrodynamics that is not always known or can be measured (easily) experimentally. The drag model studies mentioned previously used glass beads as the solid particle in the fluidized beds; however none of the drag models have been tested to validate the hydrodynamics of a fluidized bed using biomass particles. Deza et al. [8] tested the Syamlal-O'Brien and Gidaspow models for glass beads and compared with experiments. Their findings demonstrated that the Gidaspow model predictions compared well with the experiments providing confidence that the model could be used for biomass fluidization.

The goal of this research is to computationally model a cold-flow fluidized bed and to compare and validate models with experiments [4]. Initial work is pursued to study biomass fluidization using ground walnut shell and the Gidaspow drag model. In this work, the simulations of the fluidized beds will be employed using open source software Multiphase Flow with Interphase eXchanges (MFIX). The simulations will consider factors such as particle sphericity and coefficient of restitution. Results from the simulations will be compared with the particle distribution, bed height, and pressure drop obtained from the experiments.

NUMERICAL MODEL

A multifluid Eulerian-Eulerian model is employed in Multiphase Flow with Interphase eXchanges (MFIX) [9] and assumes that each phase behaves as interpenetrating continua with its own physical properties. The instantaneous variables are averaged over a region that is larger than the particle spacing but smaller than the flow domain. Volume fractions are introduced to track the fraction each phase occupies in the averaging volume, where ε_g is the gas phase volume fraction (also referred to as the void fraction) and ε_{sm} is the solid phase volume fraction for the mth solid phase. The volume fractions must satisfy the relation:

$$\varepsilon_g + \sum_{m=1}^{M} \varepsilon_{sm} = 1 \qquad (1)$$

For a mixture of particles, each distinct particle type to be modeled is represented as a solid phase m for a total of M phases. Each solid phase is described with an effective particle diameter d_p and characteristic material properties, and a conservation equation is solved for each solid phase.

The continuity equations for the gas phase and the solids phases, respectively, are:

$$\frac{\partial}{\partial t}(\varepsilon_g \rho_g) + \nabla \cdot (\varepsilon_g \rho_g \mathbf{u}_g) = \sum_{n=1}^{N_g} R_{gn} \qquad (2)$$

$$\frac{\partial}{\partial t}(\varepsilon_{sm}\rho_{sm}) + \nabla \cdot (\varepsilon_{sm}\rho_{sm}\mathbf{u}_{sm}) = \sum_{n=1}^{N_{sm}} R_{smn} \qquad (3)$$

The subscripts g and s indicate the gas and solid phases, respectively, and n denotes a unique species. Other variables include the density (ρ), velocity vector ($\mathbf{u}$) and the rate of formation (R) that models interphase mass transfer associated with chemical reactions or physical processes. For the simulations in this study, the right-hand side of Eqns. 2 and 3 are set to zero.

The momentum equations for the gas and solids phases have the form:

$$\frac{\partial}{\partial t}(\varepsilon_g\rho_g\mathbf{u}_g) + \nabla \cdot (\varepsilon_g\rho_g\mathbf{u}_g\mathbf{u}_g) = \nabla \cdot \sigma_g + \sum_{m=1}^{M} \mathbf{I}_{gm} + \varepsilon_g\rho_g\mathbf{g} \quad (4)$$

$$\frac{\partial}{\partial t}(\varepsilon_{sm}\rho_{sm}\mathbf{u}_{sm}) + \nabla \cdot (\varepsilon_{sm}\rho_{sm}\mathbf{u}_{sm}\mathbf{u}_{sm}) = \nabla \cdot \sigma_{sm} - \mathbf{I}_{gm}$$
$$+ \sum_{\substack{m=1 \\ l \neq m}}^{M} \mathbf{I}_{ml} + \varepsilon_{sm}\rho_{sm}\mathbf{g} \qquad (5)$$

The expressions on the left side are the net rate of momentum generation and the net rate of momentum transfer by convection. The right side includes contributions for the stress tensors (σ), gravity ($\mathbf{g}$), the interaction force ($\mathbf{I}_{gm}$) accounting for the momentum transfer between the gas phase and the mth solids phases, and the interaction force ($\mathbf{I}_{ml}$) between the mth and l^{th} solids phases. Kinetic theory for granular flow is used to calculate the solid stress tensor and solid-solid interaction forces in the rapid granular flow regime [9].

Based on kinetic theory, the granular temperature for the solid phases is introduced. The granular temperature θ_m can be related to the granular energy, defined as the specific kinetic energy of the random fluctuating component of the particle velocity:

$$\frac{3}{2}\theta_m = \frac{1}{2} <\mathbf{C}_m^2> \qquad (6)$$

and the fluctuation in the particle velocity is $\mathbf{C}_m = \mathbf{u}_m - \mathbf{u}_{sm}$, where $\mathbf{u}_m$ is the instantaneous translational particle velocity and the symbol $< >$ designates the operation of taking an average. The resulting transport equation for the granular temperature is:

$$\frac{3}{2}[\frac{\partial}{\partial t}(\varepsilon_{sm}\rho_{sm}\rho_{sm}) + \nabla \cdot (\varepsilon_{sm}\rho_{sm}\rho_{sm})\mathbf{u}_{sm}] =$$
$$\sigma_{sm} : \nabla\mathbf{u}_{sm} - \nabla \cdot \mathbf{q}_{\theta_m} + \gamma_{\theta_m} + \phi_{gm} \qquad (7)$$

where $\mathbf{q}_{\theta_m}$ is the diffusive flux of granular energy, γ_θ is the rate of granular energy dissipation due to inelastic collisions [10] and, ϕ_{gm} is the transfer of granular energy between the gas phase and the m_{th} solids phase.

Since the numerical simulations will model a cold-flow fluidized bed, the energy equation will not be employed in MFIX and therefore is not presented here.

Drag Modeling

The interaction force ($\mathbf{I}_{gm}$) in the momentum Eqns. 4 and 5 mainly accounts for three different mechanisms of interaction: bouyancy, drag force, and momentum transfer due to mass transfer, where:

$$\mathbf{I}_{gm} = -\varepsilon_{sm}\nabla P_g - F_{gm}(\mathbf{u}_{sm} - \mathbf{u}_g) + R_{0m}[\xi_{0m}\mathbf{u}_{sm} - \xi_{0m}\mathbf{u}_g] \quad (8)$$

The first term on the right-hand side of Eqn. 8 models buoyancy due to the fluid pressure gradient; the second term represents the drag force and is caused by the differences in velocity between the phases; and the third term corresponds to the momentum transfer due to mass transfer. The drag force is expressed as the product of the coefficient for the interphase force between the fluid phase and the mth solid phase (F_{gm}) and the slip velocity between the two phases ($\mathbf{u}_{sm} - \mathbf{u}_g$). The coefficient for the interphase force is different for each drag model.

Gidaspow model

The Gidaspow model [11] calculates the interphase drag force coefficient using two correlations depending on the void fraction value. For void fractions less than 0.8 the Ergun equation is used to calculate the interphase force coefficient and for void fractions greater than or equal to 0.8 the Wen-Yu equation is used. To avoid a discontinuity between the models, a blend function φ_{gs} is introduced:

$$\varphi_{gs} = \frac{\arctan[150 \times 1.75(0.2 - (1 - \varepsilon_g))]}{\pi} + 0.5 \qquad (9)$$

The interphase drag force for the Gidaspow model is expressed as:

$$F_{gm} = (1 - \varphi_{gs})F_{gm(Ergun)} + \varphi_{gs}F_{gm(Wen-Yu)} \qquad (10)$$

where F_{gm} for the Ergun equation valid for $\varepsilon_g < 0.8$ is:

$$F_{gm(Ergun)} = 150\frac{(1 - \varepsilon_g)^2\mu_g}{\varepsilon_g d_p^2} + 1.75\frac{(1 - \varepsilon_g)\rho_g}{d_p}|\mathbf{u}_{sm} - \mathbf{u}_g| \quad (11)$$

and F_{gm} for the Wen-Yu equation valid for $\varepsilon_g \geq 0.8$ is:

$$F_{gm(Wen-Yu)} = \frac{3}{4}C_D\frac{(1 - \varepsilon_g)\rho_g}{d_p}|\mathbf{u}_{sm} - \mathbf{u}_g|\varepsilon_g^{-2.65} \qquad (12)$$

where the drag coefficient (C_D) is expressed as:

$$C_D = \frac{24}{\varepsilon_g Re_m}\left[1 + 0.15(\varepsilon_g Re_m)^{0.687}\right] \qquad (13)$$
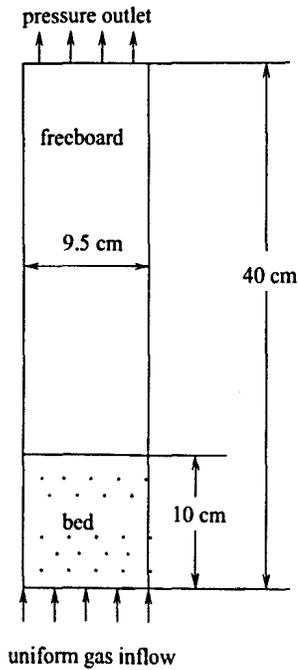
Figure 1. Schematic of the 2-D plane representing the bed chamber of the cylindrical reactor.

	Walnut Shells
d_p (cm)	0.062
ρ_p (g/cm^3)	1.30
ρ_b (g/cm^3)	0.62
ψ (–)	0.5, 0.6, 0.7
e (cm/s^2)	0.75, 0.85, 0.95
U_{mf}(cm/s)	18.7
ε_g^* (–)	0.522
U_g (cm/s)	24.3

Numerical Methodology

To discretize the governing equations in MFIX, a finite volume approach for a staggered grid is used to reduce numerical instabilities and ensure global conservation of mass and momentum [12]. Velocities are stored at the cell surfaces, and scalars, such as void fraction and pressure, are stored at the center of the cell. Discretization of time derivatives are first-order and discretization of spatial derivatives are second-order. A modification of the SIMPLE algorithm is used to solve the governing equations [12]. It should be noted that the MFIX code uses a variable time-stepping scheme to assist with convergence.

Domain Specification

The cylindrical reactor for the cold-flow experiments [4] is modeled as a two–dimensional (2-D) plane representing the centerplane of the cylinder with a 9.52 cm diameter and 40 cm height, as shown in Fig. 1. A Cartesian coordinate system is used to capture the random bubble dynamics characteristic of fluidized beds, and [13] have validated the accuracy of a 2-D approach. A uniform inlet velocity is specified at the bottom equal to the superficial gas velocity and atmospheric pressure is specified at the exit. The no-slip condition is used to model the walls of the domain for all phases.

Of particular concern is the coefficient of restitution (e) and sphericity (ψ) of biomass. The material used to represent biomass is ground walnut shell because it tends to fluidize uniformly. Table 1 summarizes the particle properties and flow conditions in this study. The packed bed height for all cases is 10 cm.

CASES AND RESULTS
Grid Resolution Study

Of particular interest to this study is the use of a robust drag model that does not require à priori information. The comparisons by Deza et al. [8] indicated that the Gidaspow model is suitable for modeling fluidized beds and will be used in the parametric study to determine coefficient of restitution and particle sphericity for biomass. The advantage of the Gidaspow model is that it only requires basic particle properties such as mean diameter and density.

Walnut shell particles are used as a case study for a biomass fluidized bed. As a starting point, a qualitative comparison is made between the experiments [4] and simulations. The gas-solid distributions at approximately 10 s intervals are shown in Fig. 2. Each subfigure shows images of the radiographs on the left and numerical simulations (using $e = 0.85$ and $\psi = 0.6$) on the right. The comparisons between experiments and simulations are not at the exact same time but rather in a time frame of $\pm$ 1 second. There is a good agreement with the formation of small bubbles near the bottom that rise and coalesce forming larger bubbles toward the top of the bed. The similarities in instantaneous gas-solid distributions between the experiments and simulations provide confidence with using the Gidaspow model to predict biomass fluidization.

Pressure drop across the ground walnut shell bed was calculated for the superficial gas velocity of $1.3U_{mf} = 24.3$ cm/s for a combination of coefficients of restitution ($e = 0.75$, 0.85, and 0.95) and particle sphericity ($\psi = 0.5$, 0.6, 0.7, and 0.8) using the Gidaspow drag model. Results from the computational simulations show that for a particle sphericity of 0.8, irrespective of the
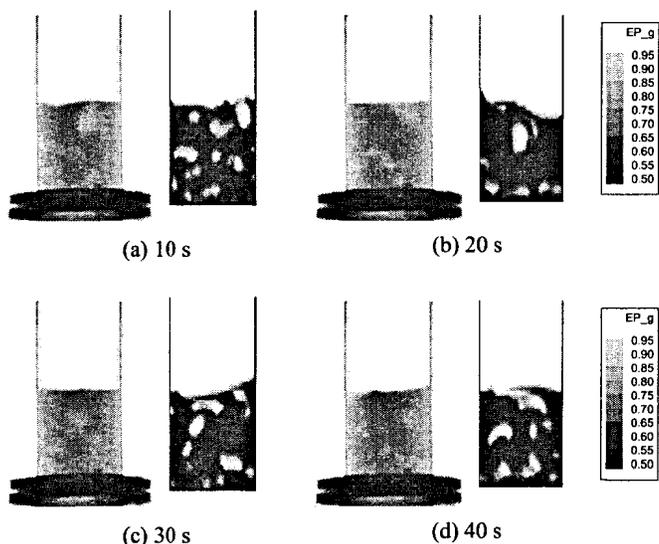
132

Figure 2: Instantaneous gas-solid distributions for the ground walnut shell fluidized bed. For each pair of images, the left side is the X-ray radiograph [4] and the right side is the void fraction contour from the simulation at (a) 10 s, (b) 20 s, (c) 30 s, and (d) 40 s.

Figure 3: Pressure drop for the ground walnut shell simulations at superficial gas velocity of $1.3U_{mf}=24.3$ cm/s and for the experiments.

coefficient of restitution, the pressure drop is 500 Pa, compared with 590 Pa for all of the other $\psi - e$ combinations and the experimentally measured value of 570 Pa. The results, shown in Fig. 3, indicate that a particle sphericity of 0.8 for ground walnut shell is not appropriate for modeling the fluidized bed.

The hydrodynamics of the bed are first analyzed to study the effects of coefficient of restitution with sphericity fixed at 0.60. The coefficient of restitution cannot be easily determined experimentally for the irregular shaped walnut shell particles; one way to find a value that best represents the actual coefficient is through a parametric study. The results should provide how sensitive the hydrodynamics are and how it affects the overall performance of the fluidized bed. Average void fraction contours from 5 to 40 seconds for the numerical simulations are shown in Fig. 4a–c for different coefficients of restitution. No considerable differences are observed between these three results. The parametric study for coefficient of restitution indicates that this variable does not have a significant influence on the bed hydrodynamics for these flow conditions, perhaps due to the lower superficial inlet gas velocity of 1.3 U_{mf}.

Another parameter tested is the biomass particle sphericity. The sphericity is the particle property that indicates how spherical a particle is, where a sphericity of unity signifies that the particle is a pecfect sphere. The coefficient of restitution is fixed at 0.85 and the superficial gas velocity is $1.3U_{mf}$.

Average void fraction contours from 5 to 40 seconds for the simulations and two perpendicular planes of the CT scan images are shown in Fig. 5. It can be seen that the particles with spheric-
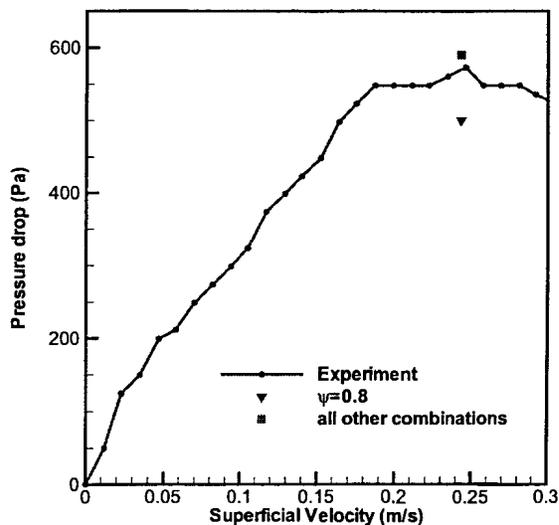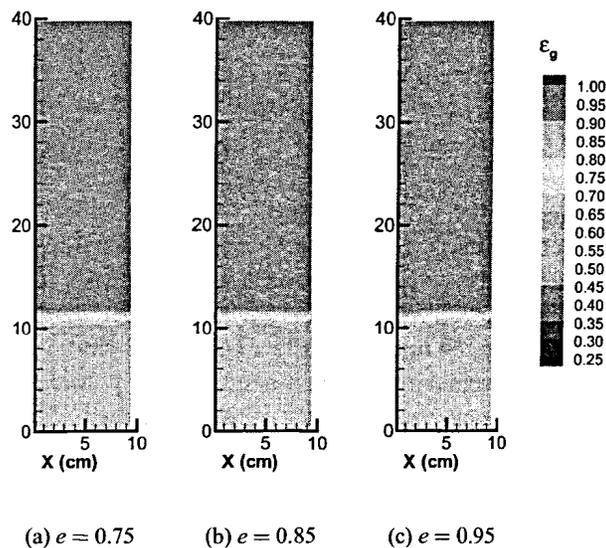

Figure 4: Average void fraction for the ground walnut shell fluidized bed using a) $e = 0.75$, (b) $e = 0.85$, and (c) $e = 0.95$; $\psi = 0.6$.

ity of 0.5 and 0.6 tend to have noticeable areas of higher concentration along the walls near $y = 8$ and 6 cm, respectively. The distribution of particles with sphericity of 0.7 is mostly constant throughout the bed. As the sphericity increases, the concentration of particles is higher in the bed and the bed height decreases. The average height of the expanded bed from the experiment is
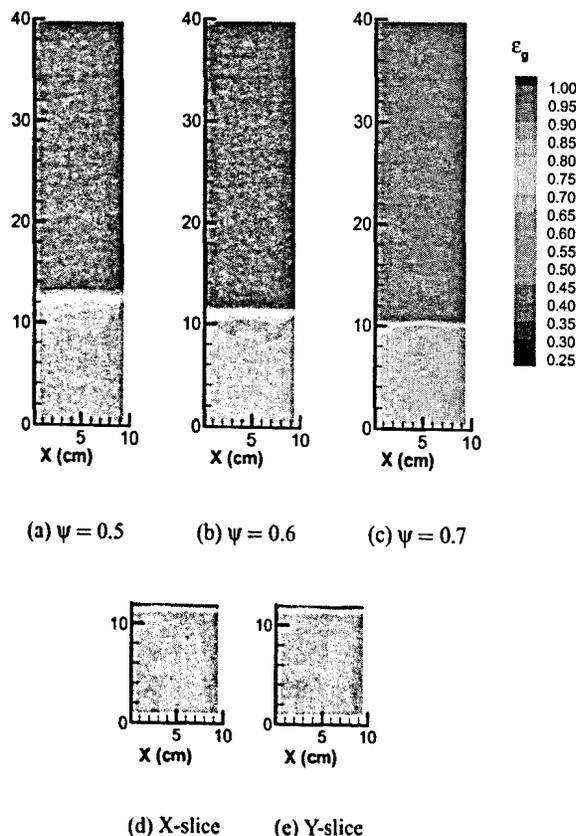
133

(a) ψ = 0.5 (b) ψ = 0.6 (c) ψ = 0.7

(d) X-slice (e) Y-slice

Figure 5: Average void fraction for the ground walnut shell simulations using a) ψ = 0.5, (b) ψ = 0.6, and (c) ψ = 0.7 and experiment CT scan images [4](d) X-slice and (e) Y-slice

11.3 cm while numerical simulations for particle sphericities of 0.5, 0.6, and 0.7 yielded an average bed height of 12.3, 11.4, and 10.3 cm respectively. A comparison of the simulations is shown in Fig. 6, which represents the void fraction averaged across the bed width versus the domain height. The sphericity parametric study indicates that sphericity does change the bed hydrodynamics and is a sensitive value in modeling biomass.

CONCLUSIONS

Ground walnut shells were used to represent biomass because the material fluidizes uniformly. Simulations of ground walnut shells were analyzed to determine parameters that can not easily be measured experimentally. Both coefficient of restitution and sphericity were varied to determine the effects on the predictions. The coefficient of restitution study showed no significant differences in the hydrodynamics of the fluidized bed for values between 0.75 and 0.95. The particle sphericity study showed that sphericity does affect the behavior of the fluidized bed. Higher sphericity values underpredict the bed hydrodynamics and bed height showing a packed bed starting to fluidize, while lower sphericities overpredict the bed hydrodynamics and
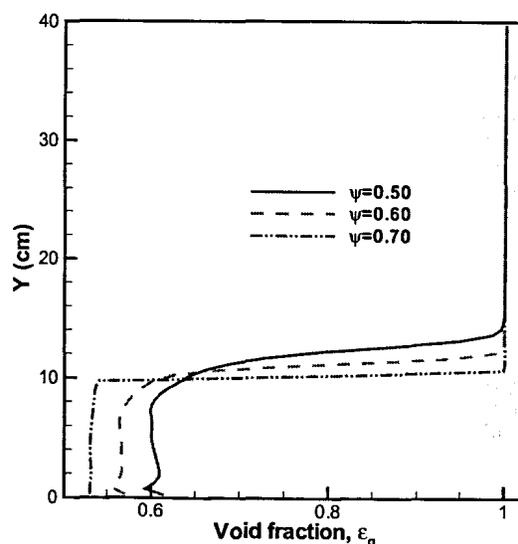

Figure 6: Void fraction for the ground walnut shell simulations averaged across the bed width versus axial direction using different particle sphericity values.

the bed height.

This research showed qualitative and quantitative comparisons of numerical and experimental data. From the parametric study it can be concluded that biomass can be modeled using the Gidaspow correlations. Furthermore, the fluidized hydrodynamics of ground walnut shell indicate that the material can be characterized with a medium sphericity ($\approx$ 0.6) and relatively large coefficient of restitution ($\approx$ 0.85). Thus, the non-uniform biomass particles tend to easily fluidize.

ACKNOWLEDGMENT

REFERENCES

[1] Heindel, T. J., Hubers, J., Jensen, T., Gray, J., and Striegel, A., 2005. Using x-rays for multiphase flow visualization. Proceedings of the 2005 ASME Fluids Engineering Division Summer Meeting and Exhibition, Houston, TX: ASME Press, Paper FEDSM2005-77359, June.

[2] Abdullah, M., Husain, Z., and Pong, S. Y., 2003. "Analysis of cold flow fluidization test results for various biomass fuels". Biomass and Bioenergy, 24(6), pp. 487–494.

[3] Hulme, I., and Kantzas, A. "Determination of bubble di-

ameter and axial velocity for a polyethylene fluidized bed using x-ray fluoroscopy". *Powder Technology,* **147**(1).

[4] Franka, N., Battaglia, F., and Heindel, T. J., 2007. Visualizing cold-flow fluidized beds with x-rays. Proceedings of the 2007 ASME International Mechanical Engineering Congress and Exposition. Paper IMECE2007-43073, November.

[5] Taghipour, F., Ellis, N., and Wong, C., 2005. "Experimental and computational study of gas-solid fluidized bed hydrodynamics". *Chemical Engineering Science,* **60**(24), December, pp. 6857–6867.

[6] Du, W., Bao, X., Xu, J., and Wei, W., 2006. "Computational fluid dynamics (cfd) modeling of spouted bed: Assessment of drag coefficient correlations". *Chemical Engineering Science,* **61**(5), March, pp. 1401–1420.

[7] Mahinpey, N., Vejahati, F., and Ellis, N. "Cfd simulation of gas-solid bubbling fluidized bed: An extensive assessment of drag models". *Computational Methods in Multiphase Flow IV: WIT Transactions on Engineering Sciences,* **56**.

[8] Deza, M., Battaglia, F., and Heindel, T. J., 2007. Computational modeling of biomass in a fluidized bed gasifier. Proceedings of the 2007 ASME International Mechanical Engineering Congress and Exposition, Seattle, WA: ASME Press, Paper IMECE2007-43097, November.

[9] Syamlal, M., Rogers, W., and O'Brien, T., 2003. MFIX documentation: Theory guide. Technical Note DOE/METC-95/1013, NTIS/DE95000031, National Energy Technology Laboratory, Department of Energy. See also URL http://www.mfix.org.

[10] Lun, C. K., Savage, S. B., Jeffrey, D. J., and Chepurniy, N. "Kinetic theory for granular flow: Inelastic particles in couette flow and slightly inelastic particles in a general flowfield". *Journal of Fluid Mechanics,* **140**.

[11] Gidaspow, D., 1994. *Multiphase Flow and Fluidization: Continuum and Kinetic Theory Descriptions.* Academy Press, Boston, USA.

[12] Syamlal, M., 1998. MFIX documentation: Numerical Technique. Technical Note DOE/MC31346-5824, NTIS/DE98002029, National Energy Technology Laboratory, Department of Energy. See also URL http://www.mfix.org.

[13] Xie, N., Battaglia, F., and Pannala, S., 2008. "Effects of using two- versus three-dimensional computational modeling of fluidized beds: Part I, hydrodynamics". *Powder Technology,* **182**(1), February, pp. 1–13.